

Bound - states for truncated Coulomb potentials

Maen Odeh and Omar Mustafa

Department of Physics, Eastern Mediterranean University

G. Magusa, North Cyprus, Mersin 10 - Turkey

email: omustafa.as@mozart.emu.edu.tr

November 2, 2018

Abstract

The pseudoperturbative shifted - l expansion technique PSLET [16-19] is generalized for states with arbitrary number of nodal zeros. Bound- states energy eigenvalues for two truncated coulombic potentials are calculated using PSLET. In contrast with shifted large-N expansion technique, PSLET results compare excellently with those from direct numerical integration.

1 Introduction

Attractive truncated Coulomb potentials

$$V(r) = -\frac{1}{(r^b + \alpha^b)^{1/b}}, \quad (1)$$

($b = 1, 2, 3, \dots$ and α is a truncation parameter) are of special physical interest. They avoid the singularity at $r = 0$ (the crux of divergence problems) and serve as models for many interesting physical phenomena [1-10]. For the case $b = 1$, Eq.(1) reads

$$V(r) = -\frac{1}{(r + \alpha)}, \quad (2)$$

the eminent cutoff Coulomb potential. In quantum-field theory, it has been suggested that if gravitational interactions of elementary particles are taken into account, there would be a gravitational cut off of Coulomb interactions resulting in a finite theory of quantum field. Eq.(2) represents therefore a nonrelativistic version of this idea. It may, moreover, be considered as an approximation of the potential of a smeared charge rather than a point charge. When $b = 2$, Eq.(1) implies

$$V(r) = -\frac{1}{(r^2 + \alpha^2)^{1/2}}, \quad (3)$$

often called the laser-dressed Coulomb potential. A model that has been found useful for the study of the spectrum of a laser-dressed hydrogen-like atoms when exposed to an intensive non-resonant laser-field [5-10]. It has been shown that under Kramers-Henneberger canonical transformations the potential of such atoms can be recast into (3) with the truncation parameter α is related to the strength of the irradiating laser field [7-9]. The effective potential for scattering by a uniform spherical charge distribution is well

simulated by (3). Moreover, it is very similar to the modified potential of the nucleus of a muonic atom due to finiteness in its size [5,11-15].

As the Schrödinger equation for neither of the potentials is amenable to a general analytic solution, one has to retain perturbation techniques or numerical methods to analyze their bound states. Mehta and Patil [2] had investigated analytically the s-state energy for the potential (2); however, no numerical results were obtained. Intensive analysis had been carried out by De Meyer and Vanden Berghe [3] and Fernandez [4] on the bound states of (2). The shifted $1/N$ expansion technique had been employed to calculate the energy eigenvalues of potential (3) [6]. David Singh et al [5] have employed a numerical method to calculate the energy eigenvalues for the potentials (2) and (3). As such, these potentials are good candidates to be analyzed through an analytical (often semi-analytical) technique to resolve their underlying physical aspects.

Recently, we have introduced a pseudoperturbative shifted- l (l is the angular momentum quantum number) expansion technique (PSLET) to solve for nodeless states of Schrödinger equation. It simply consists of using $1/\bar{l}$ as a pseudoperturbation parameter, where $\bar{l} = l - \beta$, and β is a suitable shift. The shift β is vital for it removes the poles that would emerge, at lowest orbital states with $l = 0$, in our proposed expansion below. Our new analytical, often semi-analytical, methodical proposal PSLET has been successfully applied to quasi-relativistic harmonic oscillator [16], spiked harmonic oscillator [17], anharmonic oscillators [18], and two dimensional hydrogenic atom in an arbitrary magnetic field [19].

Encouraged by its satisfactory performance in handling nodeless states, we generalize PSLET recipe (in section 2) for states with arbitrary number of nodal zeros, $n_r \geq 0$. In section 3 we apply PSLET to treat the potentials (2) and (3) and we compare the results obtained by PSLET with the exact

ones. We conclude in section 4.

2 Method

The prescription of our technique starts with the radial part of the time-independent Schrödinger equation in $\hbar = m = 1$ units,

$$\left[-\frac{1}{2} \frac{d^2}{dr^2} + \frac{l(l+1)}{2r^2} + V(r) \right] \Psi_{n_r, l}(r) = E_{n_r, l} \Psi_{n_r, l}(r). \quad (4)$$

where l is the angular momentum quantum number, $n_r = 0, 1, \dots$ counts the nodal zeros and $V(r)$ is an arbitrary spherically symmetric potential that supports bounded states.

Most textbook perturbation techniques manipulate the potential term to introduce a perturbing expansion parameter. To the contrary, our method keeps the potential arbitrary to the condition of being well-behaved. We invest the centrifugal term to play this role. Thus, with $\bar{l} = l - \beta$ (β to be determined in the sequel), Eq.(4) reads

$$\left\{ -\frac{1}{2} \frac{d^2}{dr^2} + \frac{\bar{l}^2 + (2\beta + 1)\bar{l} + \beta(\beta + 1)}{2r^2} + V(r) \right\} \Psi_{n_r, l}(r) = E_{n_r, l} \Psi_{n_r, l}(r), \quad (5)$$

Apparently, the natural limit of Eq.(5) is the large- l limit. At that limit the centrifugal term dominates over the kinetic energy and the potential terms. This results in a semiclassical motion of the particle in an effective potential $V_{eff} = \frac{1}{2r^2} + \frac{1}{Q}V(r)$, where Q is a constant that scales the potential at large- l limit and is set, for any specific choice of l and n_r , equal to \bar{l}^2 at the end of calculations[19,20]. Hence, the motion is concentrated about the minimum of V_{eff} , say r_0 . Consequently, a coordinate transformation through

$$x = \bar{l}^{1/2}(r - r_0)/r_0, \quad (6)$$

will be in point. It worths mentioning that the scaled coordinates, Eq.(6), has no effect on the energy eigenvalues, which are coordinates independent. It just facilitates the calculations of both the energy eigenvalues and eigenfunctions. Performing the coordinate transformation, Eq.(6), Eq. (5) reads

$$\left[-\frac{1}{2} \frac{d^2}{dx^2} + \frac{r_o^2}{\bar{l}} \tilde{V}(x(r)) \right] \Psi_{n_r, l}(x) = \frac{r_o^2}{\bar{l}} E_{n_r, l} \Psi_{n_r, l}(x), \quad (7)$$

$$\tilde{V}(x(r)) = \frac{\bar{l}^2 + (2\beta + 1)\bar{l} + \beta(\beta + 1)}{2r_o^2 \left(1 + \frac{x}{\sqrt{\bar{l}}}\right)^2} + \frac{\bar{l}^2}{Q} V(x(r)) \quad (8)$$

Expansions about $x = 0$, i.e. $r = r_0$, yield

$$\frac{1}{r_o^2 \left(1 + \frac{x}{\sqrt{\bar{l}}}\right)^2} = \sum_{n=0}^{\infty} (-1)^n \frac{(n+1)}{r_o^2} x^n \bar{l}^{-n/2}, \quad (9)$$

$$V(x(r)) = \sum_{n=0}^{\infty} \left(\frac{d^n V(r_o)}{dr_o^n} \right) \frac{(r_o x)^n}{n!} \bar{l}^{-n/2} \quad (10)$$

Apparently, the expansions in (9) and (10) center the problem at the point r_0 and the derivatives, in effect, contain information not only at r_0 but also at any point on the axis, in accordance with Taylor's theorem. It is also convenient to expand E as

$$E_{n_r, l} = \sum_{n=-2}^{\infty} E_{n_r, l}^{(n)} \bar{l}^{-n}. \quad (11)$$

Equation (7) thus becomes

$$\left[-\frac{1}{2} \frac{d^2}{dx^2} + \frac{r_o^2}{\bar{l}} \tilde{V}(x(r)) \right] \Psi_{n_r, l}(x) = r_o^2 \left(\sum_{n=-2}^{\infty} E_{n_r, l}^{(n)} \bar{l}^{-(n+1)} \right) \Psi_{n_r, l}(x), \quad (12)$$

with

$$\begin{aligned}
\frac{r_o^2}{\bar{l}} \tilde{V}(x(r)) &= r_o^2 \bar{l} \left[\frac{1}{2r_o^2} + \frac{V(r_o)}{Q} \right] + \bar{l}^{1/2} \left[-x + \frac{V'(r_o)r_o^3 x}{Q} \right] \\
&+ \left[\frac{3}{2}x^2 + \frac{V''(r_o)r_o^4 x^2}{2Q} \right] + (2\beta + 1) \sum_{n=1}^{\infty} (-1)^n \frac{(n+1)}{2} x^n \bar{l}^{-n/2} \\
&+ r_o^2 \sum_{n=3}^{\infty} \left[(-1)^n \frac{(n+1)}{2r_o^2} x^n + \left(\frac{d^n V(r_o)}{dr_o^n} \right) \frac{(r_o x)^n}{n!Q} \right] \bar{l}^{-(n-2)/2} \\
&+ \beta(\beta + 1) \sum_{n=0}^{\infty} (-1)^n \frac{(n+1)}{2} x^n \bar{l}^{-(n+2)/2} + \frac{(2\beta + 1)}{2}, \quad (13)
\end{aligned}$$

where the prime of $V(r_o)$ denotes derivative with respect to r_o . Equation (12) is exactly of the type of Schrödinger equation for one - dimensional anharmonic oscillator

$$\left[-\frac{1}{2} \frac{d^2}{dx^2} + \frac{1}{2} \Omega^2 x^2 + \xi_o + P(x) \right] X_{n_r}(x) = \lambda_{n_r} X_{n_r}(x), \quad (14)$$

where $P(x)$ is a perturbation - like term and ξ_o is a constant. A simple comparison between Eqs.(12), (13) and (14) implies

$$\xi_o = \bar{l} \left[\frac{1}{2} + \frac{r_o^2 V(r_o)}{Q} \right] + \frac{2\beta + 1}{2} + \frac{\beta(\beta + 1)}{2\bar{l}}, \quad (15)$$

$$\begin{aligned}
\lambda_{n_r} &= \bar{l} \left[\frac{1}{2} + \frac{r_o^2 V(r_o)}{Q} \right] + \left[\frac{2\beta + 1}{2} + (n_r + \frac{1}{2})\Omega \right] \\
&+ \frac{1}{\bar{l}} \left[\frac{\beta(\beta + 1)}{2} + \lambda_{n_r}^{(0)} \right] + \sum_{n=2}^{\infty} \lambda_{n_r}^{(n-1)} \bar{l}^{-n}, \quad (16)
\end{aligned}$$

and

$$\lambda_{n_r} = r_o^2 \sum_{n=-2}^{\infty} E_{n_r,l}^{(n)} \bar{l}^{-(n+1)}, \quad (17)$$

Equations (15) and (16) yield

$$E_{n_r,l}^{(-2)} = \frac{1}{2r_o^2} + \frac{V(r_o)}{Q} \quad (18)$$

$$E_{n_r,l}^{(-1)} = \frac{1}{r_o^2} \left[\frac{2\beta + 1}{2} + (n_r + \frac{1}{2})\Omega \right] \quad (19)$$

$$E_{n_r,l}^{(0)} = \frac{1}{r_o^2} \left[\frac{\beta(\beta + 1)}{2} + \lambda_{n_r}^{(0)} \right] \quad (20)$$

$$E_{n_r,l}^{(n)} = \lambda_{n_r}^{(n)} / r_o^2 ; \quad n \geq 1. \quad (21)$$

Here r_o is chosen to minimize $E_{n_r,l}^{(-2)}$, i. e.

$$\frac{dE_{n_r,l}^{(-2)}}{dr_o} = 0 \quad \text{and} \quad \frac{d^2E_{n_r,l}^{(-2)}}{dr_o^2} > 0, \quad (22)$$

which in turn gives, with $\bar{l} = \sqrt{Q}$,

$$l - \beta = \sqrt{r_o^3 V'(r_o)}. \quad (23)$$

Consequently, the second term in Eq.(13) vanishes and the first term adds

a constant to the energy eigenvalues. It should be noted that energy term $\bar{l}^2 E_{n_r, l}^{(-2)}$ is the energy of a particle moving under the effect of V_{eff} . Hence, it is, roughly, the energy of a classical particle with angular momentum $L_z = \bar{l}$ executing circular motion of radius r_o in the potential $V(r_o)$. This term thus identifies the leading - order approximation, to all eigenvalues, as a classical approximation and the higher - order corrections as quantum fluctuations around the minimum r_o , organized in inverse powers of \bar{l} .

The next leading correction to the energy series, $\bar{l} E_{n_r, l}^{(-1)}$, consists of a constant term and the exact eigenvalues of the unperturbed harmonic oscillator potential $\Omega^2 x^2/2$. The shifting parameter β is determined by choosing $\bar{l} E_{n_r, l}^{(-1)} = 0$. This choice is physically motivated. It requires not only the agreements between PSLET eigenvalues and the exact known ones for the harmonic oscillator and Coulomb potentials but also between the eigenfunctions as well. Hence

$$\beta = - \left[\frac{1}{2} + (n_r + \frac{1}{2})\Omega \right], \quad (24)$$

where

$$\Omega = \sqrt{3 + \frac{q_o V''(r_o)}{V'(r_o)}}. \quad (25)$$

Equation (13) thus becomes

$$\frac{r_o^2}{\bar{l}} \tilde{V}(x(r)) = r_o^2 \bar{l} \left[\frac{1}{2r_o^2} + \frac{V(r_o)}{Q} \right] + \sum_{n=0}^{\infty} v^{(n)}(x) \bar{l}^{-n/2}, \quad (26)$$

where

$$v^{(0)}(x) = \frac{1}{2} \Omega^2 x^2 + \frac{2\beta + 1}{2}, \quad (27)$$

$$v^{(1)}(x) = -(2\beta + 1)x - 2x^3 + \frac{r_o^5 V'''(r_o)}{6Q} x^3, \quad (28)$$

and for $n \geq 2$

$$v^{(n)}(x) = (-1)^n (2\beta + 1) \frac{(n+1)}{2} x^n + (-1)^n \frac{\beta(\beta+1)}{2} (n-1) x^{(n-2)} + B_n x^{n+2}, \quad (29)$$

$$B_n = (-1)^n \frac{(n+3)}{2} + \frac{r_o^{(n+4)}}{Q(n+2)!} \frac{d^{n+2}V(r_o)}{dr_o^{n+2}} \quad (30)$$

Equation (12) thus becomes

$$\left[-\frac{1}{2} \frac{d^2}{dx^2} + \sum_{n=0}^{\infty} v^{(n)} \bar{l}^{-n/2} \right] \Psi_{n_r, l}(x) = r_o^2 \left[\sum_{n=1}^{\infty} E_{n_r, l}^{(n-1)} \bar{l}^{-n} \right] \Psi_{n_r, l}(x) \quad (31)$$

Up to this point, one would conclude that the above procedure is nothing but an animation of the eminent shifted large-N expansion (SLNT) [19,20]. However, because of the limited capabilities of SLNT in handling large -order corrections via the standard Rayleigh-Schrödinger perturbation theory, only low-order corrections have been reported, sacrificing in effect its preciseness. Therefore, one should seek for an alternative and proceed by setting the wave functions with any number of nodes as

$$\Psi_{n_r, l}(x) = F_{n_r, l}(x) \exp(U_{n_r, l}(x)) \quad (32)$$

Eq.(31) is readily transformed into the following Riccati type equation

$$\begin{aligned}
& -\frac{1}{2} \left[F''_{n_r,l}(x) + 2F'_{n_r,l}(x)U'_{n_r,l}(x) \right] + F_{n_r,l}(x) \left\{ -\frac{1}{2}[U''_{n_r,l}(x) + (U'_{n_r,l}(x))^2] \right. \\
& \left. + \frac{1}{2}(2\beta + 1) + \frac{1}{2}\Omega^2 x^2 + \sum_{n=1}^{\infty} v^{(n)}(x)\bar{l}^{-n/2} \right\} = r_0^2 F_{n_r,l}(x) \sum_{n=1}^{\infty} E_{n_r,l}^{(n-1)} \bar{l}^{-n}
\end{aligned} \tag{33}$$

where primes denotes derivatives with respect to x . It is evident that (33) admits solutions of the form

$$F_{n_r,l}(x) = x^{n_r} + \sum_{n=0}^{\infty} \sum_{p=0}^{n_r-1} a_{p,n_r}^{(n)} x^p \bar{l}^{-n/2} \tag{34}$$

$$U'_{n_r,l}(x) = \sum_{n=0}^{\infty} U_{n_r}^{(n)}(x) \bar{l}^{-n/2} + \sum_{n=0}^{\infty} G_{n_r}^{(n)}(x) \bar{l}^{-(n+1)/2}, \tag{35}$$

where

$$U_{n_r}^{(n)}(x) = \sum_{m=0}^{n+1} D_{m,n,n_r} x^{2m-1} \quad ; \quad D_{0,n,n_r} = 0, \tag{36}$$

$$G_{n_r}^{(n)}(x) = \sum_{m=0}^{n+1} C_{m,n,n_r} x^{2m}. \tag{37}$$

Clearly the nodal zeros of the wavefunctions are taken care of by $F_{n_r,l}(x)$. For nodeless states,

$$F_{0,l}(x) = 1 \tag{38}$$

which reduces (33) to the problem described in our previous work for nodeless states[16-19]. To illustrate how our method works for nodal states, we will

treat the one-node state. Upon substituting equations (34)-(37) with $n_r = 1$ into (33), it reads

$$\begin{aligned}
& F_{1,l}(x) \left[-\frac{1}{2} \sum_{n=0}^{\infty} \left(U_1^{(n)'}(x) \bar{l}^{-n/2} + G_1^{(n)'}(x) \bar{l}^{-(n+1)/2} \right) \right. \\
& -\frac{1}{2} \sum_{n=0}^{\infty} \sum_{m=0}^n \left(U_1^{(m)}(x) U_1^{(n-m)}(x) \bar{l}^{-n/2} + G_1^{(m)}(x) G_1^{(n-m)}(x) \bar{l}^{-(n+2)/2} \right. \\
& \left. \left. + 2U_1^{(m)}(x) G_1^{(n-m)}(x) \bar{l}^{-(n+1)/2} \right) + \sum_{n=0}^{\infty} v^{(n)}(x) \bar{l}^{-n/2} - r_0^2 \sum_{n=1}^{\infty} E_{n_r,l}^{(n-1)} \bar{l}^{-n} \right] \\
& - F_{1,l}'(x) \left(\sum_{n=0}^{\infty} U_{n_r}^{(n)}(x) \bar{l}^{-n/2} + \sum_{n=0}^{\infty} G_{n_r}^{(n)}(x) \bar{l}^{-(n+1)/2} \right) - \frac{1}{2} F_{1,l}''(x) = 0
\end{aligned} \tag{39}$$

The solution of (39) then follows from the uniqueness of power series representation . Therefore equating the coefficients of same powers of \bar{l} and x respectively, (of course, the other way around works equally well), one gets

$$D_{1,0,1} = -\omega, \quad a_{0,1}^{(0)} = 0, \quad U_1^{(0)}(x) = -\omega x, \tag{40}$$

$$C_{1,0,1} = -\frac{B_1}{\omega}, \quad a_{0,1}^{(1)} = -\frac{C_{1,0,1}}{\omega}, \tag{41}$$

$$C_{0,0,1} = \frac{1}{\omega} (2C_{1,0,1} + 2\beta + 1), \tag{42}$$

$$D_{2,2,1} = \frac{1}{\omega} \left(\frac{C_{0,0,1}^2}{\omega} - B_2 \right) \tag{43}$$

$$D_{1,2,1} = \frac{1}{\omega} \left(\frac{5}{2} D_{2,2,1} + C_{0,0,1} C_{1,0,1} - \frac{3}{2} (2\beta + 1), \right) \tag{44}$$

$$E_{1,l}^{(0)} = \frac{1}{r_0^2} \left(\beta(\beta + 1) + a_{0,1}^{(1)} C_{1,0,1} - \frac{3D_{1,2,1}}{2} - \frac{C_{0,0,1}^2}{2} \right) \tag{45}$$

.... and so on. Obviously, one can calculate the energy eigenvalue and eigenfunctions from the knowledge of C_{m,n,n_r} , D_{m,n,n_r} and $a_{p,n_r}^{(n)}$ in a hierarchical manner. Nevertheless, the procedure just described is suitable for a software

package such as MAPLE to determine the energy eigenvalue and eigenfunction up to any order of the pseudoperturbation series.

Although the energy series Eq.(11), could appear divergent, or at best, asymptotic for small \bar{l} , one can still calculate the eigen series to a very good accuracy by performing the sophisticated [N,M] Pade' approximation[22],

$$P_N^M(1/\bar{l}) = \frac{(P_0 + P_1/\bar{l} + \dots + P_M/\bar{l}^N)}{(1 + q_1/\bar{l} + \dots + q_N/\bar{l}^M)} \quad (46)$$

to the energy series, Eq(11). The energy series, Eq(11), is calculated up to $E_{n_r,l}^{(8)}/\bar{l}^8$ by

$$E_{n_r,l} = \bar{l}^2 E_{n_r,l}^{(-2)} + E_{n_r,l}^{(0)} + \dots + E_{n_r,l}^{(8)}/\bar{l}^8 + O(1/\bar{l}^9), \quad (47)$$

and with the $P_4^4(1/\bar{l})$ Pade' approximant it becomes

$$E_{n_r,l}[4, 4] = \bar{l}^2 E_{n_r,l}^{(-2)} + P_4^4(1/\bar{l}). \quad (48)$$

Our technique is therefore well prescribed.

3 Truncated Coulomb potentials

In this section we consider the truncated Coulomb potentials, Eqs.(2) and (3).

Substituting Eq.(2) into Eq.(25), one gets

$$\Omega = \sqrt{\frac{r_0 + 3\alpha}{r_0 + \alpha}} \quad (49)$$

Eq.(23) together with Eq.(24) give then

$$l + \frac{1}{2} \left[1 + (2n_r + 1) \sqrt{\frac{r_0 + 3\alpha}{r_0 + \alpha}} \right] = \frac{r_0^{3/2}}{(r_0 + \alpha)} \quad (50)$$

When substituting Eq.(3) into Eq.(25), one gets

$$\Omega = \sqrt{\frac{r_0^2 + 4\alpha^2}{r_0^2 + \alpha^2}} \quad (51)$$

Eq.(23) in turn gives

$$l + \frac{1}{2} \left[1 + (2n_r + 1) \sqrt{\frac{r_0^2 + 4\alpha^2}{r_0^2 + \alpha^2}} \right] = \frac{r_0^2}{(r_0 + \alpha)^{3/4}} \quad (52)$$

Eqs.(50) and (52) are explicit equations in r_0 . Clearly, closed - form solutions of Eqs.(49)-(51) for r_0 are hard to be found (which is often the case). Thus, we use numerical methods to resolve the issue (hence the notion that PSLET is often semianalytical). Once r_0 is determined the coefficients $C_{m,n,n_r}, D_{m,n,n_r}, a_{p,n_r}^{(n)}$ are determined in a sequential manner. Hence the eigenvalues, Eq.(47), and eigenfunctions Eqs.(34)-(37), are calculated in the same batch for each value of l, n_r , and α .

Tables 1 and 2 show PSLET results, Eq.(47), E_{PSLET} , for $1s, 2s, 2p, 3p, 3d, 4d$ and $4f$ eigenstates of Eq.(1), covering weak, intermediate and strong ranges of the truncation parameter α . In addition, we display the Pade' approximants, Eq. (48), $E[4, 4]$, and the exact results, E_{exact} , obtained by direct numerical integration [5]. Comparing E_{PSLET} with E_{exact} , one notices the underlying relation between the accuracy of PSLET results and l, n_r and the truncation parameter, α . The accuracy of PSLET results increases with increasing l and/or n_r (See figure (2)). This is in accordance with our choice for the expansion parameter in Eq.(47), as $1/\bar{l}$ gets smaller as l and/or n_r increases. PSLET results show a good converging trend to the exact values as the truncation parameter gets larger (See figure (1)). In the strong range of α , PSLET results are almost exact. To resume the eigenenergy series, Eq. (47), Pade' approximant is calculated. Moreover, the stability noticed in different order Pade' approximants show that the results are accurate up to

ten digits at strong range of α , to the contrary of the of the results obtained in [5] where the accuracy is recorded up to eight digits in the same range.

Table 3 displays PSLET results, E_{PSLET} , for some excited states of Eq.(3) along with the Pade' approximants, $E[4, 4]$, of E_{PSLET} , the results obtained by SLNT[6], E_{SLNT} and the exact results, E_{exact} , obtained by direct numerical integration [5]. Apparently, the accuracy of our results for this potential have similar behavior as in the previous case. When compared with the results obtained by SLNT, our results show a better agreement with the exact ones. The difficulty in calculating high order corrections in SLNT through Rayleigh-Schrödinger perturbation theory results in loss in accuracy. PSLET makes it amenable to calculate high order corrections which improves the accuracy.

Moreover, one notices that the results of PSLET are more accurate in the case of the truncated coulomb potential than that of the laser-dressed one. The reason behind this is that the truncated potential is more coulombic in nature which makes PSLET nearer to the exact results.

4 Concluding remarks

We have presented a generalization of our pseudoperturbative shifted - l expansion technique PSLET [16-19] to treat states with arbitrary number of nodal zeros, $n_r \geq 0$. Two truncated coulombic potentials have been treated via PSLET and very accurate energy eigenvalues are obtained.

The outstanding features of the attendant PSLET are in order.

It avoids troublesome questions as those pertaining to the nature of small parameter expansions, the trend of convergence to the exact numerical values (marked in tables 1-3), the utility in calculating the eigenvalues and

eigenfunctions in one batch to sufficiently higher orders, and the applicability to a wide range of potentials. Moreover, beyond its promise as being quite handy, on computational and practical methodical sides, it offers a useful perturbation prescription where the zeroth- order approximation inherits a substantial amount of the total energy.

Finally, the scope of PSLET applicability extends beyond the present truncated coulombic potentials. It could be applied to angular momentum states of multi - electron atoms [23-25], relativistic and non relativistic quark - antiquark models [26], etc. We believe that the feature of our method in determining expressions for the bound-state wavefunctions makes it possible to describe electron transitions and multiphoton emission occurring in atomic systems in the presence of an intense laser field. It is therefore reasonable to re-examine such phenomena in the frame work of PSLET.

References

- [1] Patil H.1981 Phys. Rev. A**24** 2913
- [2] Mehta H. and Patil H 1978 Phys. Rev A**17** 43
- [3] Meyer De and Berghe G. V. 1990 J Phys A **23** 1323
- [4] Fernandez F M 1991 J Phys A**24** 1351
- [5] Singh D., Varshni Y P and . Dutt R 1985 Phys Rev A **32** 619
- [6] Dutt R., Mukherji U and Varshni Y P 1985 J Phys B: At. Mol. Phys. **18** 3311 (and references there in)
- [7] Miranda L C 1981 Phys Lett A**86** 363
- [8] Lima C A and Miranda L C 1981 Phys Lett A **86** 367
- [9] Lima C A and Miranda L C 1981 Phys Rev A **23** 3335
- [10] Landgraf T C et al 1982 Phys Lett A **92**, 131
- [11] Landau L, ” Niels Bohr and the Development of Physics ”, Oergamon, London (1956); O Klein, ibid.
- [12] Pauli W 1956 Helv. Phys. Acta. Suppl. **4** 69
- [13] DeserS 1957 Rev. Mod. Phys. **29** 417
- [14] Isham C J, Salam A and StrathdeeJ 1971 Phys. Rev. D **3** 1805 ; 1972 **5**, 2548
- [15] Marshak R E, ” Meson Physics ”, Dover, New York, 1952.
- [16] Mustafa O and Odeh M 1999 J. Phys. A**32** 6653

- [17] Mustafa O and Odeh M 1999 J. Phys B**32** 3055
- [18] Mustafa O and Odeh M, Eur. Phys. J Bxx (in press)
- [19] Mustafa O and Odeh M, Commun. Theor. Phys. xx (in press).
- [20] Imbo T, Pagnamenta A and Sukhmate U 1984 Phys. Rev D**29** 1669 .
- [21] Maluendes S A, Fernandez F M and Castro E A 1989 Phys. Lrta A**39** 1605
- [22] Bender C M and Orszag S A 1978 " *Advanced Mathematical Methods for Scientists and Engineers*" (McGraw- Hill, New York).
- [23] Dunn M and Watson D 1996 Few - Body Systems **21** 187
- [24] Dunn M and Watson D 1996 Ann Phys **251** 266
- [25] Dunn M and Watson D 1999 Phys. Rev A**59** 1109
- [26] Lichtenberg D et al. 1990 Z Phys. C**46** 75

Table1. Bound-state energies, in $\hbar = m = 1$ units, of the potential $V(r) = -\frac{1}{(r + \alpha)}$ for the $1s$, $2s$, $2p$ and $3p$ states. E_{PSLET} represents PSLET results, Eq (47), E_{44} is the [4,4] Pade' approximant, Eq. (48), and E_{exact} from direct numerical integration [5].

	α	$1s$	$2s$	$2p$	$3p$
$-E_{PSLET}$	0.1	0.387357746	0.109481497	0.117535370	0.053309085
$-E_{44}$		0.387922157	0.109145059	0.117535388	0.053309210
$-E_{exact}$		0.38754365	0.10950805	0.11753535	0.05330930
	1.0	0.180406651	0.069577091	0.082862488	0.041787781
		0.180368972	0.069581801	0.082862452	0.041787655
		0.18036705	0.06958066	0.08286242	0.04178766
	10	0.043439053	0.024810349	0.029446519	0.018748152
		0.043438645	0.024810342	0.029446516	0.018748153
		0.04343872	0.02481036	0.02944652	0.01879815
	50	0.012194732	0.008579236	0.009717589	0.007237436
		0.012194683	0.008579235	0.009717588	0.007237436
		0.01219469	0.00857924	0.00971759	0.00723744
	200	0.003653176	0.002907080	0.003169533	0.002608781
		0.003653168	0.002907080	0.003169533	0.002608781
		0.00365317	0.00290708	0.00316953	0.00260878

Table2. Bound-state energies, in $\hbar = m = 1$ units, of the potential $V(r) = -\frac{1}{(r + \alpha)}$ for the $3d$, $4d$ and $4f$ states. E_{PSLET} represents PSLET results, Eq (47), E_{44} is the [4,4] Pade' approximant, Eq. (48), and E_{exact} from direct numerical integration [5].

	α	$3d$	$4d$	$4f$
$-E_{PSLET}$	0.1	0.054136568	0.030648450	0.030813599
$-E_{44}$		0.054136568	0.030648449	0.030813599
$-E_{exact}$		0.05413657	0.03064845	0.03081360
	1.0	0.045010006	0.026625065	0.027588160
		0.045010007	0.026625059	0.027588160
		0.04501001	0.02662506	0.02758816
	10	0.021024302	0.014373461	0.015576600
		0.021024302	0.014373461	0.015576600
		0.02102430	0.01437346	0.01557660
	50	0.007962796	0.006153630	0.006643882
		0.007962796	0.006153630	0.006643882
		0.00796280	0.00615363	0.00664388
	200	0.002798562	0.002353647	0.002498272
		0.002798562	0.002353647	0.002498272
		0.00279856	0.00235365	0.00249827

Table3. Bound-state energies, in $\hbar = m = 1$ units, of the potential $V(r) = -\frac{1}{(r^2 + \alpha^2)^{1/2}}$ for the $3d$, $4d$ and $4f$ states. E_{PSLET} represents PSLET results, Eq (47), E_{44} is the [4,4] Pade' approximant, Eq. (48), E_{SLNT} is from SLNT [6] and E_{exact} from direct numerical integration [5].

	α	$2s$	$3p$	$4d$
$-E_{PSLET}$		0.121234415	0.055496250	0.031244807
$-E_{44}$	0.1	0.126937229	0.055498046	0.031244799
$-E_{SLNT}$	—	—	—	—
$-E_{exact}$		0.12182090	0.05549523	0.03124480
	1.0	0.089679150	0.052114869	0.030781155
		0.095048845	0.052110018	0.030781125
		0.089903	0.052509	0.030838
		0.09267933	0.05206038	0.03078150
	10	0.037161915	0.028313951	0.021412017
		0.037154303	0.028313599	0.021412537
		0.037111	0.028225	0.021353
		0.03715440	0.02831369	0.02141257
	50	0.012450958	0.010878999	0.009476019
		0.012450960	0.010879000	0.009476018
		0.016263	0.010882	0.009477
		0.01245096	0.01087900	0.00947602
	200	0.003923030	0.003659489	0.003410238
		0.003923030	0.003659489	0.003410238
		0.004503	0.003660	0.003411
		0.00392303	0.00365949	0.00341024

(a)

(b)

(c)

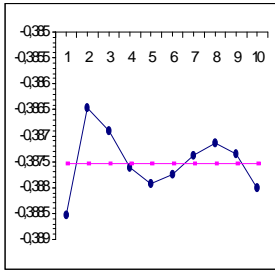
Figure(1): The effect of the truncation parameter on the trend of convergence of Eq.(47) for 1s-state of Eq.(2): (a) $\alpha = 0.1$, (b) $\alpha = 50$, (c) $\alpha = 200$. Where the numbers on the horizontal axis represent the number of corrections added to the leading energy term of PSLET, Eq.(47), the vertical axis represents the energies (in $\hbar = m = 1$ units) and the horizontal curve denotes the exact numerical results from [5].

(a)

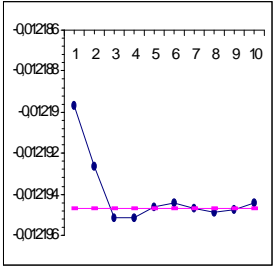
(b)

(c)

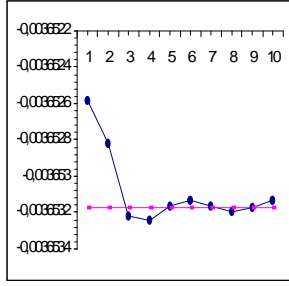
Figure(2): The effect of the angular momentum quantum number, l , and the radial quantum number, n_r , on the convergence trend of Eq.(47) for (2) with $\alpha = 50$: (a) 1s-state , (b) 3p-state , (c) 4d-state. The figures prescription is similar to figure 1.



(a)

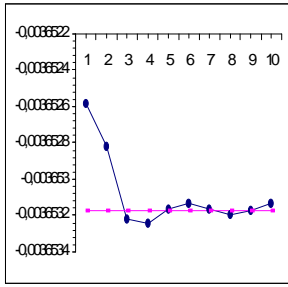


(b)

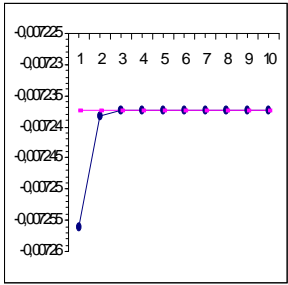


(c)

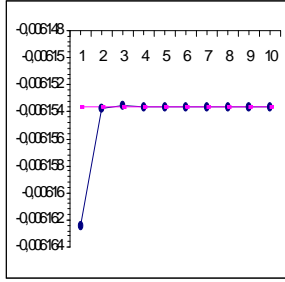
Figure(1): The effect of the truncation parameter on the trend of convergence of Eq.(47) for 1s-state of Eq.(2): (a) $\alpha = 0.1$, (b) $\alpha = 50$, (c) $\alpha = 200$. Where the numbers on the horizontal axis represent the number of corrections added to the leading energy term of PSLET, Eq.(47), the vertical axis represents the energies (in $\hbar = m = 1$ units) and the horizontal curve denotes the exact numerical results from [5].



(a)



(b)



(c)

Figure(2): The effect of the angular momentum quantum number, l , and the radial quantum number, n_r , on the convergence trend of Eq.(47) for (2) with $\alpha = 50$: (a) 1s-state , (b) 3p-state , (c) 4d-state. The figures prescription is similar to figure 1.